# Spectral dispersion of the linewidth enhancement factor and four wave mixing conversion efficiency of an InAs/GaAs multimode quantum dot laser 🄴🄿

🆔 Shihao Ding, 🆔 Bozhang Dong, Heming Huang, et al.

**COLLECTIONS**

🄴🄿　This paper was selected as an Editor's Pick

View Online　　Export Citation　　CrossMark

**ARTICLES YOU MAY BE INTERESTED IN**

Broadband, efficient extraction of quantum light by a photonic device comprised of a metallic nano-ring and a gold back reflector
Applied Physics Letters **120**, 081103 (2022); https://doi.org/10.1063/5.0082347

A perspective on optimizing photoelectric conversion process in 2D transition-metal dichalcogenides and related heterostructures
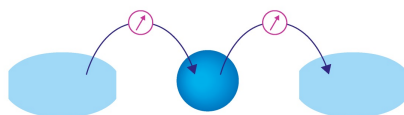Applied Physics Letters **120**, 080501 (2022); https://doi.org/10.1063/5.0079346

Improved LED output power and external quantum efficiency using InGaN templates
Applied Physics Letters **120**, 081104 (2022); https://doi.org/10.1063/5.0084273

# Spectral dispersion of the linewidth enhancement factor and four wave mixing conversion efficiency of an InAs/GaAs multimode quantum dot laser ᴱᴾ

Shihao Ding,[1] 🄳 Bozhang Dong,[1] 🄳 Heming Huang,[1] John Bowers,[2] and Frédéric Grillot[1,3,a]

## AFFILIATIONS

[1]LTCI, Télécom Paris, Institut Polytechnique de Paris, 19 Place Marguerite Perey, Palaiseau 91120, France
[2]Institute for Energy Efficiency, University of California, Santa Barbara, California 93106, USA
[3]Center for High Technology Materials, University of New Mexico, 1313 Goddard St. SE, Albuquerque, New Mexico 87106, USA

[a]Author to whom correspondence should be addressed: frederic.grillot@telecom-paristech.fr

## ABSTRACT

The spectral dependence of the linewidth enhancement factor ($\alpha_H$-factor) of a multimode InAs/GaAs quantum dot laser is analyzed. Amplified spontaneous and high-frequency modulation methods are used to experimentally retrieve the $\alpha_H$-factor of each longitudinal mode below and above the threshold. A dispersion of the $\alpha_H$-factor is unlocked across the entire optical spectrum, which is further illustrated in the context of four wave mixing experiments. The results show that the induced conversion efficiency is increased at lasing wavelengths where the linewidth enhancement is lower. These results highlight the importance of carefully monitoring the linewidth enhancement factor in quantum dot lasers especially for frequency combs and mode-locking applications in future optical communication systems.

*Published under an exclusive license by AIP Publishing.* https://doi.org/10.1063/5.0077221

Owing to the strong carrier confinement and discrete energy levels, quantum dot (QD) lasers have demonstrated excellent performance, such as low threshold current, high temperature stability, and strong reflection insensitivity. In addition, these light sources offer broad gain bandwidth, narrow spectral linewidth, and low relative intensity noise that is highly desired for silicon integrated technologies and optical frequency comb (OFC) applications.[1–7] An OFC typically consists of equally spaced discrete optical frequency components, which is of first importance in high-capacity optical communication systems. Due to the aforementioned properties, integrated comb QD sources are particularly attractive for wavelength-division multiplexing (WDM) systems, thanks to the size and power consumption advantages wherein a low linewidth, a wide tunable comb spacing, and a high power per comb line are expected.[8,9] Therefore, a single comb spectrum can be used to replace hundreds of individual lasers with the goal to decrease the energy consumption and to scale down the size of the WDM communication system.

When studying the nonlinear and dynamic properties of a semiconductor laser, an important gain-medium parameter to consider is the linewidth enhancement factor ($\alpha_H$-factor) that is defined as follows:

$$\alpha_H = -2k \frac{d\delta n}{dN} \times \left( \frac{dG}{dN} \right)^{-1}, \qquad (1)$$

where $\delta n$ is the carrier-induced refractive index, $G$ is the gain, $N$ is the carrier density, and $k$ is the lasing wavevector. The $\alpha_H$-factor governs many coherent processes in semiconductor lasers. In particular, a prior work revealed that frequency comb dynamics of a QD laser are strongly impacted by four-wave mixing (FWM) through the $\alpha_H$-factor while another one linked that parameter to the onset of a giant Kerr nonlinearity and frequency modulated combs.[10,11] It was also shown that the $\alpha_H$ can produce a low-threshold multimode instability and frequency comb formation. In this context, the precise knowledge of the dispersion of the linewidth enhancement factor across an entire optical spectrum has become a crucial factor to better analyze the role that this parameter has on the frequency comb dynamics.[12] The $\alpha_H$-factor can be measured by several methods.[13–16] Some measurements techniques give access to the material $\alpha_H$, whereas some other reflect the device $\alpha_H$. Below the lasing threshold, the amplified spontaneous emission (ASE) is commonly used to extract the spectral dependent material $\alpha_H$-factor. It relies on measuring the net modal gain change and tracking the wavelength shift at different sub-threshold bias

currents.[4,17–19] The measurements of $\alpha_H$ above threshold rely on other measurement methods, such as those using optical injection or high-frequency modulation. In the former, the accuracy in the $\alpha_H$ extraction is limited because the injection ratio needs to be relatively low in order to protect the laser from the injected field.[20,21] The latter relies on high-frequency laser current modulation, which generates both amplitude modulation (AM) and frequency modulation (FM). The ratio of the FM over AM components gives a direct access to the linewidth enhancement factor if and only if the modulation frequency is larger than the laser's corner frequency.[13] This measurement method produces highly reliable data; however, its applicability is usually restricted to single-mode lasers.[13,22] In order to investigate multimode QD lasers, an optical phase modulation (OPM) method can be considered instead. In such way, the sinusoidal OPM signal is used to obtain the information of the longitudinal modes, hence giving access to the spectral dependence of the device $\alpha_H$.[10,23,24]

In this Letter, this spectral dispersion of the $\alpha_H$ is investigated in a multimode InAs/GaAs QD laser. To do so, both ASE and OPM measurement techniques are used to track the $\alpha$ parameter of each longitudinal mode below and above the threshold. A clear dispersion of the $\alpha_H$-factor is observed across the entire optical spectrum. In addition, four wave mixing (FWM) experiments using an intracavity drive probe configuration reveal a clear increase in the conversion efficiency as the linewidth enhancement factor decreases. Overall, these results highlight the importance of carefully monitoring the $\alpha_H$-factor in QD lasers especially with the view of using such light sources for optical frequency combs in future information and communication systems.

The active region of the QD laser consists of 8 InAs QD layers directly grown on a GaAs wafer in a solid source molecular beam epitaxy system. A 37.5 nm thick GaAs barrier layer is added between each QD layers. The density of QDs is as high as $5.9 \times 10^{10}$ cm$^{-2}$ to provide a high gain. The laser is 750 $\mu$m long with a 2 $\mu$m wide ridge waveguide. Asymmetric reflection facets of 30% at the front and 90% at the rear are coated. The device studied exhibits sole ground state (GS) emission at 1310 nm. Figure 1 displays the multimode lasing spectrum for the QD laser at 25 mA.
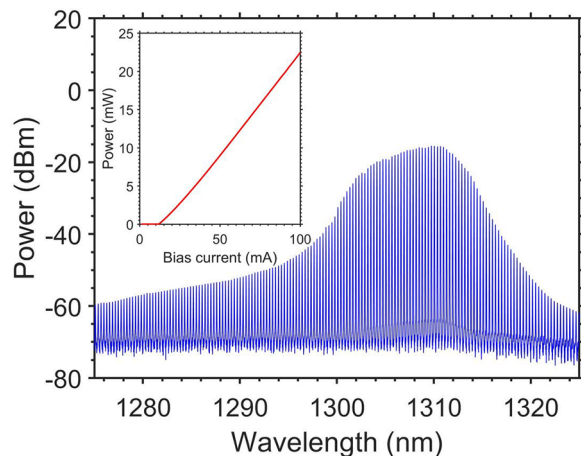
Let us note that the excited state (ES) transition is not visible in the range of pump current under study. The figure in the inset shows the light current characteristics with a threshold current $I_{th}$ of 12.5 mA. During the whole experiment, the QD laser is kept at a constant operating temperature of 20 °C.
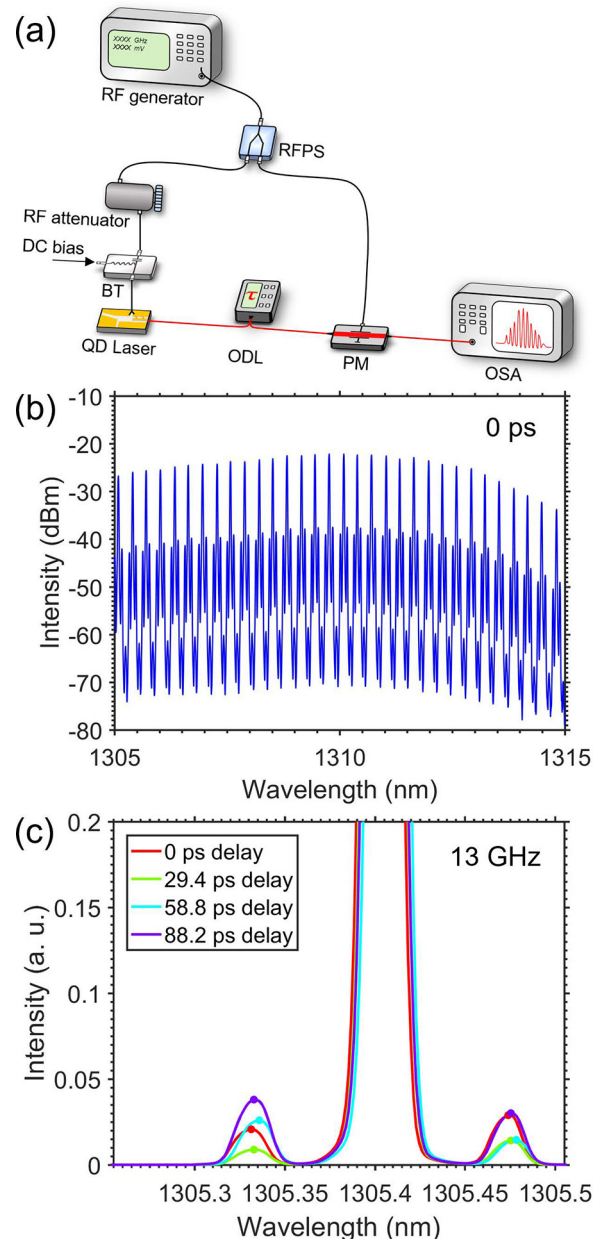


FIG. 2. (a) Schematic of the experimental setup of the OPM technique. PM, phase modulator; ODL, optical delay line; OSA, optical spectrum analyzer; BT, bias tee; RFPS, RF Power Splitter. The black line is the circuit, and the red line is the light path. (b) Modulated optical spectrum at zero delay with $f_m = 13$ GHz, and (c) close-up on one longitudinal mode and the modulation side bands obtained for four different optical delays.



FIG. 1. Optical spectrum measured at twice threshold current, and the inset shows power–current characteristics.

Figure 2(a) presents the experimental setup used for performing the extraction of the $\alpha_H$-factor with the OPM. Details regarding the ASE method are already described elsewhere. To start, the tunable RF signal (with modulation frequency $f_m$) is divided into two channels by a RF Power Splitter (RFPS) and used to simultaneously modulate the QD laser and phase modulator (PM). The sinusoidal wave signal applied to the QD laser is controlled by the RF variable attenuator to keep it within the small signal modulation. In addition, the bias tee (BT) allows the QD laser to be pumped by direct current. The laser beam is coupled with an antireflection (AR) coated lens-end fiber and then passes through an optical delay line (ODL) before entering the PM to control the delay between the optical and electrical signal at the input of the PM. Finally, the modulated signal is sent to an optical spectrum analyzer (OSA). In this method, four optical spectra corresponding to different delays [$n/(4f_m)$, with $n$ an integer] are used to properly extract the $\alpha_H$-factor.

Figure 2(b) depicts the modulated spectrum for $f_m = 13\,\text{GHz}$ and zero delay. It can be seen that the whole spectrum is affected by the modulation leading to side-modes arising at each comb line. In order to further analyze the impact of the delay on the modulation spectrum, Fig. 2(c) shows a close-up on one longitudinal mode and the modulation sidebands obtained for four different optical delays (normalized optical spectrum). When the delay is changed, the corresponding intensities are modified and can be measured directly from the OSA. According to the below expressions, the modulation frequency-dependent $\alpha_m$ can be extracted as follows:[23]

$$\alpha_m = \frac{Im\left(\sqrt{Q_{-1}Q_{+1}}\right)}{Re\left(\sqrt{Q_{-1}Q_{+1}}\right)}, \tag{2}$$

with

$$Q_{-1} = (I_{-1}^1 - I_{-1}^3) + j(I_{-1}^0 - I_{-1}^2), \tag{3}$$

$$Q_{+1} = (-I_{+1}^1 + I_{+1}^3) + j(I_{+1}^0 + I_{+1}^2), \tag{4}$$

where $I_{\pm 1}^n$ means the side-modes intensity when the optical delay is $n/(4f_m)$ ($n = 0, 1, 2, 3$). Finally, it is known that the modulation $\alpha_m$ is related to the corner frequency ($f_c$) and the modulation frequency ($f_m$),[13]

$$\alpha_m = \alpha_H \sqrt{1 + \left(\frac{f_c}{f_m}\right)^2}, \tag{5}$$

where the $f_c$ is defined as $f_c = (v_g P/2\pi) \times (\delta g/\delta P)$, where $v_g$ is the group velocity, $P$ is the output power, and $\delta g/\delta P$ is a nonzero parameter due to the nonlinear gain associated with coulomb scattering and carrier heating (CH). According to Eq. (4), when $f_m \gg f_c$, the $\alpha_H$-factor can be accurately extracted.

Figures 3(a)–3(c) display the optical spectra and the retrieved $\alpha_m$ for 18 comb lines under different modulation frequencies at $\times 2$, $\times 4$, and $\times 6$ threshold current. The extracted $\alpha_m$ shows a linear upward trend as the lasing wavelength increases over a large bandwidth range. On the one hand, the $\alpha_m$ increases with the pump current, which has already been reported elsewhere.[10] On the other hand, under the same
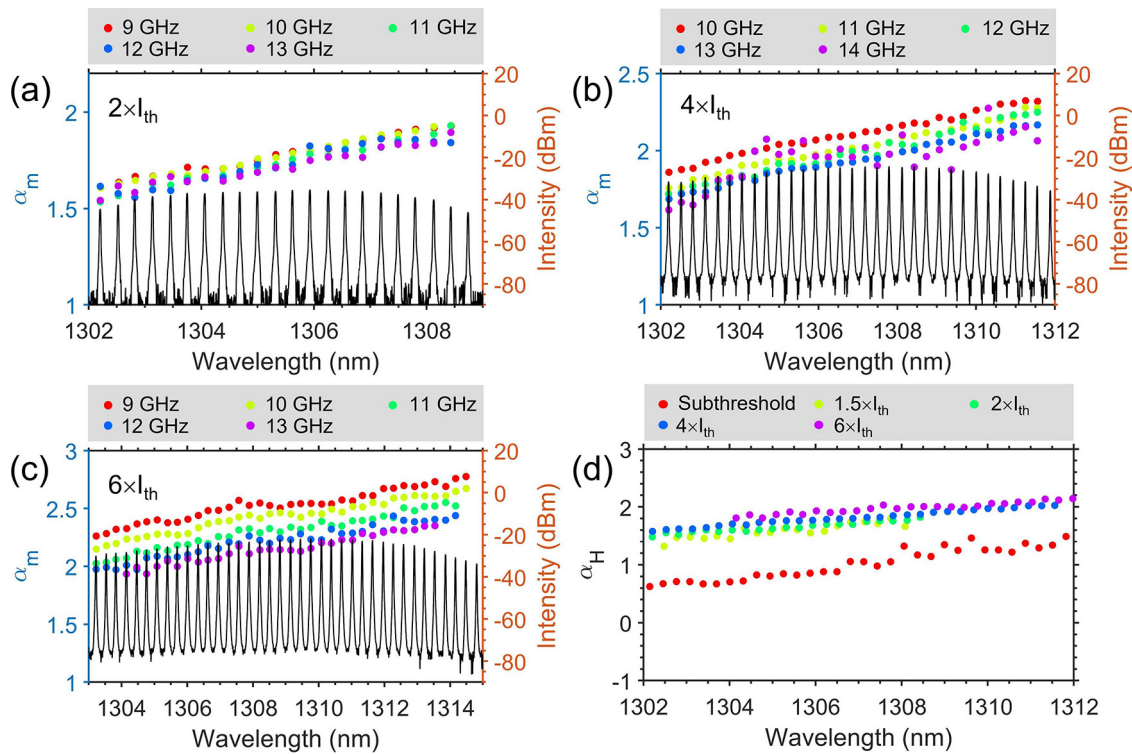


**FIG. 3.** (a) The $\alpha_m$ factor measured for each comb line for different modulation frequencies and at $\times 2$ threshold current, (b) $\times 4$ threshold current, and (c) $\times 6$ threshold current, and (d) the $\alpha_H$-factor for different pump currents extracted from the OPM and ASE methods.

pump current, the $\alpha_m$ decreases with the modulation frequency increasing from 9 to 13 GHz. Such an effect can be explained by Eq. (5). It is worth stressing that the influence of modulation frequency is amplified at high bias conditions, where $f_c$ is increased. In addition, it has been shown that the longitudinal modes located far away from the optical gain peak are less efficiently modulated by the sidebands, which results in an inaccuracy to extract the $\alpha_H$-factor. To overcome this issue, a flat-top behavior is required for the optical spectra. Owing to the broad 10 dB bandwidth emitted from the device studied, we can retrieve the $\alpha_H$-factors over 20 modes in this study. In this context, the OPM method is beneficial for extending its functionality to characterize frequency comb sources that have flat-top spectra.

Then, fixing the pump current and taking the $\alpha_m$ values at the gain peak for different modulation frequencies, Eq. (5) is used for curve-fitting the corner frequency and subsequently to extract the exact $\alpha_H$. Given that the accuracy to extract the $\alpha_H$-factor approaches its maximum when $f_c \ll f_m$, one take $f_m = 13$ GHz at which $\alpha_m \simeq \alpha_H$. Therefore, when the QD laser is running at twice threshold current, the $\alpha_H$-factor at the gain peak is about 1.6, whereas at four times and six times, the threshold current is about 1.8 and 2.0, respectively, as shown in Fig. 3(d). We also plot the sub-threshold $\alpha_H$-factor measured with the ASE method (red). The $\alpha_H$-factor below threshold is significantly smaller than the $\alpha_H$-factor above threshold, which is attributed to the carrier changes caused by the population inversion.[25]

A semiconductor comb laser is driven by a FWM process that exhibits a clear dependence of the $\alpha_H$-factor. In this study, we go a step further by investigating the FWM conversion efficiency under different $\alpha_H$ conditions. To this end, the injection-locking wavelength is applied to be different, where the $\alpha_H$-factor is changed with the variation of wavelength. To begin with, an intracavity drive-probe experiment is designed. As shown in Fig. 4, two narrow linewidth tunable lasers are used as drive laser and probe laser of which the light is sent

to a 90/10 fiber beam splitter and then injected into the QD laser through an optical circulator and a lens-end fiber. The polarization controllers are applied to align the polarization of the two tunable lasers with that of the QD laser in order to reach the maximum FWM conversion. The optical spectrum is recorded by an optical spectrum analyzer (OSA) having a 20 pm resolution. The operating temperature is kept at 298 K throughout the experiment using a thermoelectric cooler. The drive laser is used to lock the laser cavity modes below threshold in the presence of the side modes deeply suppressed by a factor of 30 dB, which allows for generating the FWM coherent beating. Depending on the frequency detuning $\Delta f$ that is defined as the difference between the frequency of probe and drive, the FWM is dependent on different mechanism. In the case of a low frequency detuning of a few gigahertz, the FWM is dominated by the carrier density pulsation (CDP). However, the spectral hole burning (SHB) and the carrier heating (CH) become the principle mechanism that determine the FWM behavior in the case of a large frequency detuning at terahertz range.[26–28] To obtain the maximum frequency conversion efficiency, on needs to adjust the probe signal to perfectly match one of the suppressed Fabry–Pérot (F–P) cavity modes in the stable-locking operation regime. Then, the conversion efficiency is expressed as

$$\eta = \frac{P_{Probe}}{P_{Signal}}, \qquad (6)$$

where $P_{Signal}$ is the optical power of the converted signal and $P_{Probe}$ is the probe signal power that is injected into the laser. In the experiment, these powers are obtained from the measured optical spectrum. Finally, the laser–fiber coupling loss is estimated by calculating the ratio between the laser free-space output power and the laser power coupled in the lens-end fiber. The total losses include coupling loss and fiber loss, which are considered in the spectra in order not to overestimate the value of conversion efficiency.
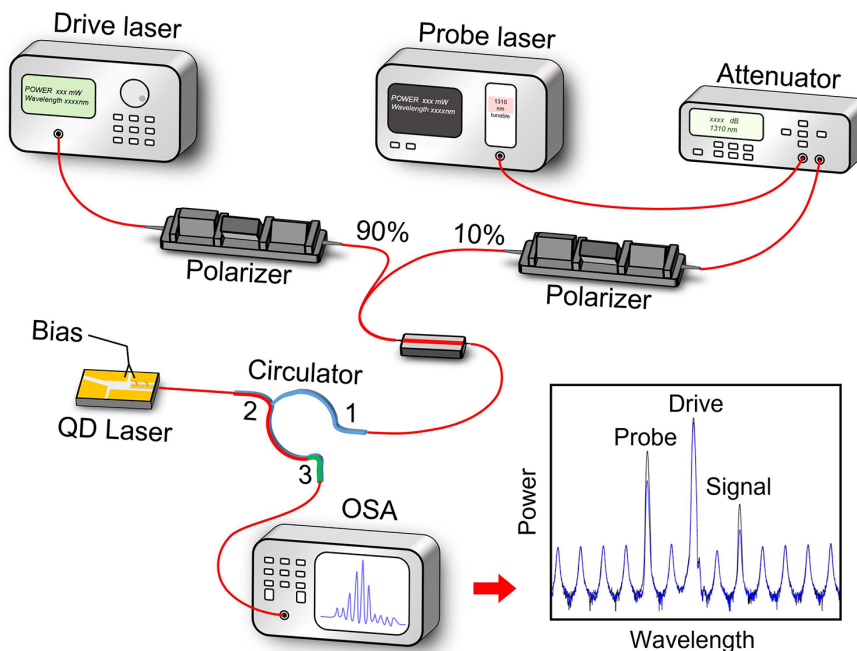


FIG. 4. Optical injection locking setup used for the FWM experiments. The drive laser is used to lock the F–P mode of the QD laser. The tunable probe laser is used to generate the probe signal. The inset shows the spectrum of FWM.

With different applied drive wavelengths, the effect of the spectral dispersion of the $\alpha_H$-factor can be qualitatively analyzed through the FWM conversion efficiencies with respect to the frequency detuning. Here, the conversion efficiency is extracted at twice the threshold of the QD laser and assuming two different drive wavelengths located on each side of the optical spectrum, namely, 1304 and 1310 nm, respectively. As the experiment is performed above the laser threshold, the device $\alpha_H$-factor measured by the PM technique is obviously considered for the analysis. Thus, Fig. 3(a) reminds that the $\alpha_H$-factor at 1304 nm is 20% smaller than that at 1310 nm. Considering a frequency detuning $\Delta f$ between the drive and the probe in the range of $\pm 500$ GHz, the conversion efficiency retrieved in the FWM regime is shown in Fig. 5 at 1304 nm (purple) and 1310 nm (orange), respectively, for both up- and down-conversions. The region where the frequency detuning is negative represents the case for upconversion, where the frequency of the probe laser is lower than the drive laser frequency. However, the positive frequency detuning region accounts for the downconversion case, where the frequency of the probe laser is higher than the drive laser frequency. At 1310 nm, the maximum conversion efficiency of $-15.6$ dB ($\alpha_H$-factor $= 2.0$) is found against $-11.5$ dB at 1304 nm ($\alpha_H$-factor $= 1.6$). Moreover, at 1304 nm, the conversion efficiency exhibits a better symmetrical shape over the whole detuning range. The $\alpha_H$-factor is indeed closely related to CDP and SHB, hence influencing the third-order nonlinear parameters and determining the symmetry of the conversion efficiency.[29] Therefore, a small $\alpha_H$-factor is beneficial for producing a higher conversion efficiency and a better symmetry between up- and down-conversions. The results show that conversion efficiency is increased at lasing wavelengths where the linewidth enhancement is smaller, which is important for understanding mode-locking and frequency comb dynamics.

To summarize, this work investigates the $\alpha_H$-factor of a multimode QD laser. We extracted the $\alpha_H$-factor below and above the threshold whereby the spectral dependence of this parameter is performed for each longitudinal mode. A dispersion of the $\alpha_H$-factor across the entire optical spectrum is observed, which is further illustrated with drive probe exper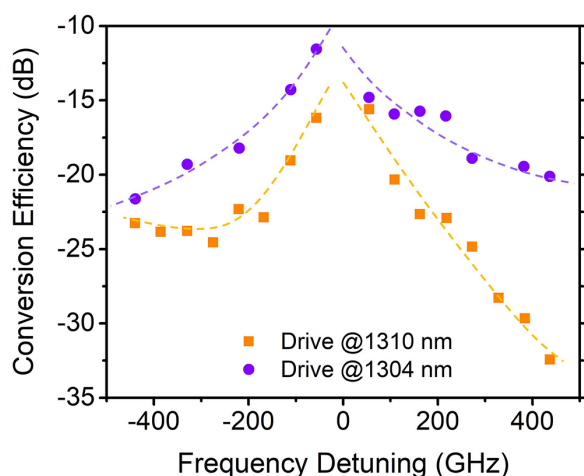iments. The results show that conversion efficiency is increased at lasing wavelengths where the linewidth enhancement is smaller. The results confirm the importance of the linewidth enhancement factor in QD lasers especially for frequency combs and mode-locking applications in future optical communication systems. Future work will focus on the $\alpha_H$-factor analysis of silicon-based quantum dot lasers and frequency comb lasers for WDM systems and their impacts on nonlinear dynamics.

## AUTHOR DECLARATIONS
### Conflict of Interest
The authors have no conflicts of interest to disclose.

### Author Contributions
S.D. and B.D. contributed equally to this work.

## DATA AVAILABILITY
The data that support the findings of this work are available from the corresponding author upon reasonable request.

## REFERENCES
[1]D. Jung, R. Herrick, J. Norman, K. Turnlund, C. Jan, K. Feng, A. C. Gossard, and J. E. Bowers, "Impact of threading dislocation density on the lifetime of InAs quantum dot lasers on Si," Appl. Phys. Lett. **112**(15), 153507 (2018).
[2]D. Arsenijević and D. Bimberg, "Quantum-dot lasers for 35 Gbit/s pulse-amplitude modulation and 160 Gbit/s differential quadrature phase-shift keying," Proc. SPIE **9892**, 98920S (2016).
[3]C. Shang, E. Hughes, Y. T. Wan, M. Dumont, R. Koscica, J. Selvidge, R. Herrick, A. C. Gossard, K. Mukherjee, and J. E. Bowers, "High-temperature reliable quantum-dot lasers on Si with misfit and threading dislocation filters," Optica **8**(5), 749–754 (2021).
[4]J. N. Duan, H. M. Huang, D. Jung, Z. Y. Zhang, J. Norman, J. E. Bowers, and F. Grillot, "Semiconductor quantum dot lasers epitaxially grown on silicon with low linewidth enhancement factor," Appl. Phys. Lett. **112**(25), 251111 (2018).
[5]B. Z. Dong, J. D. Chen, F. Y. Lin, J. Norman, J. E. Bowers, and F. Grillot, "Dynamic and nonlinear properties of epitaxial quantum-dot lasers on silicon operating under long-and short-cavity feedback conditions for photonic integrated circuits," Phys. Rev. A **103**(3), 033509 (2021).
[6]A. Y. Liu, C. Zhang, J. Norman, A. Snyder, D. Lubyshev, J. M. Fastenau, A. W. Liu, A. C. Gossard, and J. E. Bowers, "High performance continuous wave 1.3 $\mu$m quantum dot lasers on silicon," Appl. Phys. Lett. **104**(4), 041104 (2014).
[7]S. J. Pan, J. N. Huang, Z. C. Zhou, Z. X. Liu, L. Ponnampalam, Z. Z. Liu, M. C. Tang, M. C. Lo, Z. Z. Cao, K. Nishi et al., "Quantum dot mode-locked frequency comb with ultra-stable 25.5 GHz spacing between 20 °C and 120 °C," Photonics Res. **8**(12), 1937–1942 (2020).
[8]J. Norman, D. Jung, Y. T. Wan, and J. E. Bowers, "Perspective: The future of quantum dot photonic integrated circuits," APL Photonics **3**(3), 030901 (2018).
[9]J. W. Wang, F. Sciarrino, A. Laing, and M. G. Thompson, "Integrated photonic quantum technologies," Nat. Photonics **14**(5), 273–284 (2020).
[10]B. Z. Dong, J. N. Duan, H. M. Huang, J. Norman, K. Nishi, K. Takemasa, M. Sugawara, J. E. Bowers, and F. Grillot, "Dynamic performance and reflection sensitivity of quantum dot distributed feedback lasers with large optical mismatch," Photonics Res. **9**(8), 1550–1558 (2021).

**FIG. 5.** The measured conversion efficiency as a function of the frequency detuning for two injection-locking wavelengths of 1304 and 1310 nm, respectively.

[11]N. Opačak, S. D. Cin, J. Hillbrand, and B. Schwarz, "Frequency comb generation by Bloch gain induced giant Kerr nonlinearity," Phys. Rev. Lett. **127**(9), 093902 (2021).

[12]D. Burghoff, "Unraveling the origin of frequency modulated combs using active cavity mean-field theory," Optica **7**(12), 1781–1787 (2020).

[13]J. G. Provost and F. Grillot, "Measuring the chirp and the linewidth enhancement factor of optoelectronic devices with a Mach–Zehnder interferometer," IEEE Photonics J. **3**(3), 476–488 (2011).

[14]C. Henry, "Theory of the linewidth of semiconductor lasers," IEEE J. Quantum Electron. **18**(2), 259–264 (1982).

[15]M. Osinski and J. Buus, "Linewidth broadening factor in semiconductor lasers—An overview," IEEE J. Quantum Electron. **23**(1), 9–29 (1987).

[16]K. Vahala, L. C. Chiu, S. Margalit, and A. Yariv, "On the linewidth enhancement factor α in semiconductor injection lasers," Appl. Phys. Lett. **42**(8), 631–633 (1983).

[17]A. Bogatov, A. Boltaseva, A. E. Drakin, M. A. Belkin, and V. P. Konyaev, "Anomalous dispersion, differential gain, and dispersion of the α-factor in InGaAs/AlGaAs/GaAs strained quantum-well semiconductor lasers," Semiconductors **34**(10), 1207–1213 (2000).

[18]I. D. Henning and J. V. Collins, "Measurements of the semiconductor laser linewidth broadening factor," Electron. Lett. **19**(22), 927–929 (1983).

[19]J. N. Duan, H. M. Huang, B. Z. Dong, J. C. Norman, Z. Y. Zhang, J. E. Bowers, and F. Grillot, "Dynamic and nonlinear properties of epitaxial quantum dot lasers on silicon for isolator-free integration," Photonics Res. **7**(11), 1222–1228 (2019).

[20]G. Liu, X. M. Jin, and S. L. Chuang, "Measurement of linewidth enhancement factor of semiconductor lasers using an injection-locking technique," IEEE Photonics Technol. Lett. **13**(5), 430–432 (2001).

[21]D. Herrera, V. Kovanis, and L. F. Lester, "Using transitional points in the optical injection locking behavior of a semiconductor laser to extract its dimensionless operating parameters," IEEE J. Sel. Top. Quantum Electron. **28**, 21051325 (2022).

[22]C. Wang, M. E. Chaibi, H. M. Huang, D. Erasme, P. Poole, J. Even, and F. Grillot, "Frequency-dependent linewidth enhancement factor of optical injection-locked quantum dot/dash lasers," Opt. Express **23**(17), 21761–21770 (2015).

[23]J. G. Provost, A. Martinez, A. Shen, and A. Ramdane, "Single step measurement of optical transmitters henry factor using sinusoidal optical phase modulations," Opt. Express **19**(22), 21396–21403 (2011).

[24]N. Opačak, F. Pilat, D. Kazakov, S. D. Cin, G. Ramer, B. Lendl, F. Capasso, and B. Schwarz, "Spectrally resolved linewidth enhancement factor of a semiconductor frequency comb," Optica **8**(9), 1227–1230 (2021).

[25]S. Melnik, G. Huyet, and A. V. Uskov, "The linewidth enhancement factor α of quantum dot semiconductor lasers," Opt. Express **14**(7), 2950–2955 (2006).

[26]G. P. Agrawal, "Population pulsations and nondegenerate four-wave mixing in semiconductor lasers and amplifiers," J. Opt. Soc. Am. B **5**(1), 147–159 (1988).

[27]T. Akiyama, H. Kuwatsuka, N. Hatori, Y. Nakata, H. Ebe, and M. Sugawara, "Symmetric highly efficient (/spl sim/0 dB) wavelength conversion based on four-wave mixing in quantum dot optical amplifiers," IEEE Photonics Technol. Lett. **14**(8), 1139–1141 (2002).

[28]D. Nielsen and S. L. Chuang, "Four-wave mixing and wavelength conversion in quantum dots," Phys. Rev. B **81**(3), 035305 (2010).

[29]H. M. Huang, K. Schires, P. J. Poole, and F. Grillot, "Non-degenerate four-wave mixing in an optically injection-locked InAs/InP quantum dot Fabry-Perot laser," Appl. Phys. Lett. **106**(14), 143501 (2015).